Acta Pharmacol Sin 2009 Jan; 30 (1): 78–89

Original Article

# Hydrogen peroxide mobilizes $Ca^{2+}$ through two distinct mechanisms in rat hepatocytes

Hirohiko SATO[1], Teruko TAKEO[2], Qiang LIU[3], Kyoko NAKANO[2], Tomohiro OSANAI[4], Sechiko SUGA[1], Makoto WAKUI[1,#], Jie WU[3,#,*]

[1]*Department of Physiology, Hirosaki University School of Medicine, Hirosaki 036-8562, Japan;* [2]*Department of Medical Technology, Hirosaki University School of Health Sciences, Hirosaki 036-8564, Japan;* [3]*Division of Neurology, Barrow Neurological Institute, Phoenix, AZ, 85013-4496, USA;* [4]*Department of Internal Medicine, Hirosaki University School of Medicine, Hirosaki 036-8562, Japan*

**Aim:** Hydrogen peroxide ($H_2O_2$) is produced during liver transplantation. Ischemia/reperfusion induces oxidation and causes intracellular $Ca^{2+}$ overload, which harms liver cells. Our goal was to determine the precise mechanisms of these processes.

**Methods:** Hepatocytes were extracted from rats. Intracellular $Ca^{2+}$ concentrations ($[Ca^{2+}]_i$), inner mitochondrial membrane potentials and NAD(P)H levels were measured using fluorescence imaging. Phospholipase C (PLC) activity was detected using exogenous $PIP_2$. ATP concentrations were measured using the luciferin-luciferase method. Patch-clamp recordings were performed to evaluate membrane currents.

**Results:** $H_2O_2$ increased intracellular $Ca^{2+}$ concentrations ($[Ca^{2+}]_i$) across two kinetic phases. A low concentration (400 μmol/L) of $H_2O_2$ induced a sustained elevation of $[Ca^{2+}]_i$ that was reversed by removing extracellular $Ca^{2+}$. $H_2O_2$ increased membrane currents consistent with intracellular ATP concentrations. The non-selective ATP-sensitive cation channel blocker amiloride inhibited $H_2O_2$-induced membrane current increases and $[Ca^{2+}]_i$ elevation. A high concentration (1 mmol/L) of $H_2O_2$ induced an additional transient elevation of $[Ca^{2+}]_i$, which was abolished by the specific PLC blocker U73122 but was not eliminated by removal of extracellular $Ca^{2+}$. PLC activity was increased by 1 mmol/L $H_2O_2$ but not by 400 μmol/L $H_2O_2$.

**Conclusions:** $H_2O_2$ mobilizes $Ca^{2+}$ through two distinct mechanisms. In one, 400 μmol/L $H_2O_2$-induced sustained $[Ca^{2+}]_i$ elevation is mediated via a $Ca^{2+}$ influx mechanism, under which $H_2O_2$ impairs mitochondrial function via oxidative stress, reduces intracellular ATP production, and in turn opens ATP-sensitive, non-specific cation channels, leading to $Ca^{2+}$ influx. In contrast, 1 mmol/L $H_2O_2$-induced transient elevation of $[Ca^{2+}]_i$ is mediated via activation of the PLC signaling pathway and subsequently, by mobilization of $Ca^{2+}$ from intracellular $Ca^{2+}$ stores.

**Keywords:** hydrogen peroxide; $Ca^{2+}$ dynamics; non-selective cation channel; intracellular ATP; phospholipase C; hepatocyte; patch-clamp
*Acta Pharmacologica Sinica* (2009) 30: 78–89; doi: 10.1038/aps.2008.4; published online 15th December 2008

## Introduction

The development of ischemia-reperfusion injury is a major risk factor associated with liver transplantation[1–4] and coronary bypass surgery[5]. In the liver, one of the mechanisms causing ischemia-reperfusion injury seems to be oxidative stress to liver cells (hepatocytes), which occurs when pro-oxidants overwhelm cellular anti-oxidant defense mechanisms[3, 6]. Oxygen that is rapidly supplied to cells immediately following reperfusion of the liver is converted to oxygen radicals, including superoxide anions, hydroxyl radicals and hydrogen peroxide ($H_2O_2$). Subsequent oxidation by these radicals of critical proteins, DNA and lipids, and oxidation-related mitochondrial dysfunction, causes lethal damage to cells[2, 7]. Reactive oxygen and nitrogen species also are generated in the mitochondria, which then exert a toxic effect on mitochondrial function.

In oxidation-related cellular damage, an increase in intracellular $Ca^{2+}$ concentration ($[Ca^{2+}]_i$), which is likely produced by oxygen radicals, is known to accelerate cellular

# These authors played an equal role in this paper.
* Correspondence to Jie WU, MD, PhD.
E-mail Jie.Wu@chw.edu
Received 2008-07-24 Accepted 2008-09-18

damage[8, 9]. In fact, excess $Ca^{2+}$ in the cell causes cellular damage by activating $Ca^{2+}$-dependent proteases[10], although cellular $Ca^{2+}$ overload is unlikely to be the sole mechanism mediating cell death[11].

Various mechanisms by which oxygen radicals cause an elevation of $[Ca^{2+}]_i$ have been described in different types of cells. For instance, oxygen radicals induce $Ca^{2+}$ release from intracellular $Ca^{2+}$ stores in pancreatic acinar cells[12] and neutrophils[13]. In mesangial cells[14], oxygen radicals induce $Ca^{2+}$ influx from the extracellular space. In cardiac myocytes[15], an inhibition of cellular $Ca^{2+}$ extrusion or uptake seems to be responsible for the elevation of $[Ca^{2+}]_i$ induced by oxygen radicals. In addition, oxygen radicals have also been shown to be responsible for $Ca^{2+}$-dependent mitochondrial dysfunction[16] and $Ca^{2+}$ entry[17]. The $Ca^{2+}$ influx resulting from $H_2O_2$ seems to involve the Fas protein[17]. However, the precise mechanisms of $H_2O_2$-induced $[Ca^{2+}]_i$ elevation have remained elusive, and more information about the mechanisms by which $H_2O_2$ affects the $Ca^{2+}$ dynamics of hepatocytes is needed in order to develop strategies for preventing reperfusion-related hepatic injury.

In the present study, we first examined the effect of $H_2O_2$ on $[Ca^{2+}]_i$ in freshly dissociated rat hepatocytes. After confirming that $H_2O_2$ elevates $[Ca^{2+}]_i$ according to two dynamic pathways, we investigated the underlying mechanisms using multiple experimental approaches. Our techniques included patch-clamp recordings to monitor membrane currents, fluorescence imaging to examine $[Ca^{2+}]_i$ and mitochondrial function, and biochemical measurements to determine levels of PLC activity and intracellular ATP concentrations.

## Materials and methods

This study was carried out in accordance with the Guidelines for Animal Experimentation, Hirosaki University, and Guiding Principles for the Care and Use of Animals in the Field of Physiological Sciences, as approved by the Council of the Physiological Society of Japan.

**Hepatocyte dissociation** Isolated hepatocytes were prepared using a method used in a previous study[18]. Briefly, adult male rats (Wistar) were anesthetized with diethyl ether, and a perfusion catheter was inserted into the portal vein after the hepatic vein had been cut open. The perfusion solution (pH 7.4) contained (all units are mmol/L): 137 NaCl, 5.4 KCl, 0.5 $NaH_2PO_4$, 0.4 $Na_2HPO_4$, 2.0 $CaCl_2$, 4.2 $NaHCO_3$, 5 glucose and 10 HEPES. Perfusion was carried out at a rate of 20 mL/min for the first 2 min using the perfusion solution and then for another 8 min using the perfusion solution with collagenase (Type I, Wako Pure Chemical, Japan). The liver was then excised and diced into small pieces (approximately 1 $mm^3$). The specimens were subsequently incubated in the collagenase-containing solution at 37 °C for 15 min and aerated with 100% $O_2$. Afterwards, the specimens were filtered through gauze and centrifuged. In certain cases, a piece of liver tissue was removed without perfusion, diced and incubated in the collagenase-containing solution for 17 min.

**Measurement of $[Ca^{2+}]_i$** The $[Ca^{2+}]_i$ of hepatocytes was estimated using fluorescence imaging. Cells were plated onto glass coverslips coated with poly-*D*-lysine, and incubated in Williams E medium containing 10% fetal calf serum, 0.02 U/mL insulin, 10 U/mL penicillin, 10 mg/mL streptomycin, 0.05 mg/mL gentamycin, 4 mg/mL dexamethasone and 2 mmol/L glutamine. Following incubation for 2 h, the coverslips and cells were transferred into a chamber that contained a HEPES buffer extracellular solution plus 1 mmol/L Fura-2/AM (Dojin Chem, Japan) and were loaded for 30 min. Images were captured using an inverted microscope (Axiovert 135, Zeiss, Germany) with 40X Plan-Neofluar objectives and a silicon intensifier target camera. Images were recorded on a fluorescence-imaging system (Argus 50/CA, Hamamatsu Photonics, Japan). To record Fura-2 fluorescence, excitation wavelengths selected from a xenon light source were 340 and 380 nm, and the emission wavelength was 510 nm. $[Ca^{2+}]_i$ was calculated using the following formula[16]: $[Ca^{2+}]_i=K_d \beta (R-R_{min})/(R_{max}-R)$, where $R$ is the ratio of the fluorescence intensities at the two wavelengths ($F_{340}/F_{380}$), $K_d$ is the dissociation constant of Fura-2 binding to $Ca^{2+}$, and β is the maximum fluorescence at 380 nm ($F_{380\ max}$) divided by the minimal fluorescence at 380 nm ($F_{380\ min}$). The values $R_{max}$, $R_{min}$, $F_{380\ max}$, and $F_{380\ min}$ were obtained by calibration using ionomycin (Calbiochem, La Jolla, CA) and EGTA. In our system, numerical values of the coefficients were as follows: $K_d$=224 nmol/L, $R_{min}$=0.33, $R_{max}$=8.56, and β=12.52. All microfluorimetric experiments were carried out at room temperature (22±2 °C).

**Measurement of PLC activity** The PLC activity of islets was examined using a protocol utilized in previous reports[19, 20]. Liver tissues were homogenized in an ice-cold Tris-sucrose buffer (270 mmol/L sucrose buffered with 50 mmol/L Tris-HCl; pH 7.4) using a Teflon-glass homogenizer. The homogenate was centrifuged at 500×*g* for 10 min, and the pellet was discarded. The supernatant was centrifuged at 40 000×*g* for 15 min, and the pellet was washed two more times at 40 000×*g*, once in 50 mmol/L Tris-HCl buffer (pH 7.7) containing 5 mmol/L EDTA and once in EDTA-free Tris-HCl. The resulting pellets were stored at –80 °C. The protein content of the membrane fractions was

measured spectrophotometrically. The pellet containing the membrane fractions was divided into four groups, and PLC activity was measured using exogenous $PIP_2$. The following components were added to the PLC assay: 50 mmol/L HEPES (pH 7.0), 0.1 mmol/L $CaCl_2$, 9 mmol/L sodium cholate, [$^3$H]-$PIP_2$ (40,000 cpm) and membrane protein (10–40 μg/assay) in a final volume of 200 μL. To the four different groups, the following materials were further added 10 min before initiation of incubation: vehicle only, 10 μmol/L $H_2O_2$, 100 μmol/L $H_2O_2$ or 1 mmol/L $H_2O_2$. The reaction mixture was incubated for 2 min at 37 ºC. The reaction was stopped with 1 mL chloroform/methanol/concentrated HCl (100:100:0.6) followed by 0.3 mL of 1 mol/L HCl containing 5 mmol/L EGTA. After extraction, a 400-μL portion of the aqueous phase was removed for liquid scintillation counting. For determination of inositol trisphosphate ($IP_3$) in the aqueous phase, 400 μL of aqueous phase was neutralized with 133 mL of 1 mol/L NaOH, and after 15 min on ice, the precipitated perchloric acid extract was pelleted by centrifugation. One-milliliter aliquots of the neutralized supernatants were diluted with 9 mL of 5 mmol/L sodium tetraborate and applied onto pre-washed 0.8-mL columns packed with AG1X8 (200–400 mesh) formate anion exchange resin. The columns were rinsed twice with 12 mL of a 60 mmol/L sodium formate-5 mmol/L tetraborate solution, and the inositol phosphates were eluted sequentially with 1 mol/L $NH_4$ formate in 0.1 mol/L formic acid and counted using liquid scintillation.

**Measurement of inner mitochondrial membrane potential and NAD(P)H** To measure changes in inner mitochondrial membrane potentials, dissociated hepatocytes were loaded with 10 mg/mL rhodamine 123 (Rh123, Sigma) for 10 min. The Rh123 fluorescence was excited at a wavelength of 490 nm and filtered at 510 nm[21]. To further examine mitochondrial function, cellular NAD(P)H intensity (emission: 510 nm) was also measured[22].

**Measurement of ATP concentrations in hepatocytes** The levels of ATP in hepatocytes were measured using the luciferin-luciferase method[23]. Assay kits (FL-ASC) were purchased from Sigma. For the ATP assay, dissociated cells were suspended at a density of $1\times10^5$ cells/mL in the Na-HEPES buffer. Following application of $H_2O_2$, the cell samples were transferred to a reaction tube and the emission was immediately measured using a luminescence reader (BLR-301, Aloka, Japan). The bioluminescence, produced by the luciferin-luciferase reaction, was amplified and output in terms of count rate (cpm) after conversion to pulse signals.

**Patch-clamp recordings** Dissociated rat hepatocytes were kept in a 35-mm Petri dish, and the dish was placed on the stage of an inverted microscope (IMT-2, Olympus, Tokyo, Japan). The membrane currents in response to clamped voltage stimulations were measured using a patch-clamp amplifier (EPC-7, List Electronic, Darmstadt, Germany). The whole-cell configuration was established by two methods: the amphotericin B-perforation method and the conventional standard method. The inside-out patch was also used to measure the conductance of the patch membrane. The resistance of the electrodes, when filled with the pipette solution, ranged from 2 to 4 MΩ. Voltage stimulations were applied in two ways: 10 mV increasing and decreasing step pulses from the holding potential of -20 mV and ramp pulses from -90 to 80 mV using a voltage stimulator (SET-2100, Nihon Kohden, Tokyo, Japan). All electrophysiological experiments were carried out at room temperature.

**Solutions and drugs** The standard extracellular solution (pH 7.3) for measurement of $[Ca^{2+}]_i$ and electrophysiological studies contained (in mmol/L): 135 NaCl, 5.6 KCl, 1.2 $MgCl_2$, 1 $CaCl_2$, 5.5 glucose and 10 HEPES. The pipette solution (pH 7.2) used for recording whole-cell membrane currents using perforated patches contained (in mmol/L): 100 K-gluconate, 35 KCl, 0.5 EGTA, 10 HEPES, 5.5 glucose, and 240 μg/mL amphotericin B (Sigma). To obtain whole-cell recordings using the conventional method, amphotericin B was removed from the pipette solution described above and 5 mmol/L ATP was added. For inside-out patch recordings, the pipette solution contained (in mmol/L): 135 NaCl, 5.6 KCl, 1.2 $MgCl_2$, 1 $CaCl_2$, 5.5 glucose, 0.5 EGTA and 10 HEPES. The bath solution contained (in mmol/L): 100 K-gluconate, 35 KCl, 1.2 $MgCl_2$, 0.5 EGTA, 10 HEPES, 5.5 glucose and 1 ATP. $H_2O_2$ was purchased from Wako Chem, Japan, and was dissolved daily in the extracellular solution. ATP, amiloride, ouabain, melatonin and U73122 were purchased from Sigma.

**Statistics** Data are expressed as means±SD. The statistical significance of the average values was evaluated using the paired or non-paired Student's *t*-test. ANOVA was also used. A value of $P<0.05$ was considered to be significant.

## Results

**$H_2O_2$ increased $[Ca^{2+}]_i$ consistent with two kinetic patterns in rat hepatocytes** In the presence of extracellular $Ca^{2+}$ (1 mmol/L), $H_2O_2$ at concentrations below 50 μmol/L showed little effect on $[Ca^{2+}]_i$ in acutely dissociated rat hepatocytes (Figure 1A). At 100 μmol/L, $H_2O_2$ initiated a transient small drop and then gradually increased $[Ca^{2+}]_i$ (Figure 1B). At 400 μmol/L, $H_2O_2$ induced a marked elevation of $[Ca^{2+}]_i$ following a transient drop (Figure 1C).

Interestingly, a further increase in $H_2O_2$ concentration to 1 mmol/L induced a biphasic elevation of $[Ca^{2+}]_i$, including an initial transient elevation followed by a sustained elevation (Figure 1D). These results indicate that $H_2O_2$ elevates $[Ca^{2+}]_i$ in a concentration-dependent manner and suggest that these two dynamic phases of $[Ca^{2+}]_i$ elevation elicited by different concentrations of $H_2O_2$ may be mediated through different mechanisms.

**Effects of extracellular $Ca^{2+}$ on $H_2O_2$-induced biphasic elevation of $[Ca^{2+}]_i$** Initial experiments were designed to identify the possible sources of the elevation of $[Ca^{2+}]_i$ induced by $H_2O_2$. Extracellular $Ca^{2+}$ was artificially removed from the external solution by perfusion of the cell with a $Ca^{2+}$-free (plus 1 mmol/L EGTA) external solution. Under external $Ca^{2+}$-free conditions, 400 μmol/L $H_2O_2$ failed to elevate $[Ca^{2+}]_i$, but after replacing extracellular $Ca^{2+}$ (1 mmol/L), $H_2O_2$ elevated $[Ca^{2+}]_i$ (Figure 2A). Under the same $Ca^{2+}$-free conditions, 1 mmol/L $H_2O_2$ induced only a transient elevation of $[Ca^{2+}]_i$ (Figure 2B). These results suggest that 400 μmol/L $H_2O_2$ induces a sustained $[Ca^{2+}]_i$ elevation that is dependent on extracellular $Ca^{2+}$, but that 1 mmol/L $H_2O_2$-induced transient elevation of $[Ca^{2+}]_i$ is independent of extracellular $Ca^{2+}$.

**Effects of $H_2O_2$ on membrane currents of hepatocytes** Figure 2 clearly demonstrates that low concentrations (400 μmol/L) of $H_2O_2$ induce a sustained increase of $[Ca^{2+}]_i$ that is dependent on an influx of extracellular $Ca^{2+}$ into the cell. A key question concerns which $Ca^{2+}$-permeable channels and/or pathways mediate $H_2O_2$-induced $Ca^{2+}$ influx? To address this question, we measured membrane currents using patch-clamp recordings and tested the effects of $H_2O_2$ on membrane currents of rat hepatocytes. Under perforated (amphotericin B) patch-clamp recording conditions in current-clamp mode, the resting membrane potential of rat hepatocytes was between -4 and -15 mV ($n$=30), and the single-cell capacitance of hepatocytes was 9–11 pF ($n$=30). In voltage-clamp mode, whole-cell membrane currents induced by voltage-step pulses were nearly instantaneous in their onset, and current-voltage ($I$-$V$) relationships showed a slight inward rectification (Figure 3Aa, c). Bath-applied 400 μmol/L $H_2O_2$ increased voltage-step pulse-induced membrane currents (Figure 3Ab, c). The two curves obtained from $I$-$V$ relationships in the presence or absence of $H_2O_2$ crossed each other near the original membrane potential (Figure 3Ac). When conventional whole-cell patch-clamp recordings were performed (with 5 mmol/L ATP in the pipette solution), 400 μmol/L $H_2O_2$ failed to increase voltage-step pulse-induced membrane currents (Figure 3Bb, c), suggesting that $H_2O_2$ (400 μmol/L) increased voltage-step pulse-induced membrane currents likely via a reduction of intracellular ATP.

**ATP-sensitive non-specific cation channels in rat hepatocytes** The results shown in Figure 3 suggest that $H_2O_2$-induced enhancement of membrane current is dependent on intracellular substances, likely ATP. To test this hypothesis,

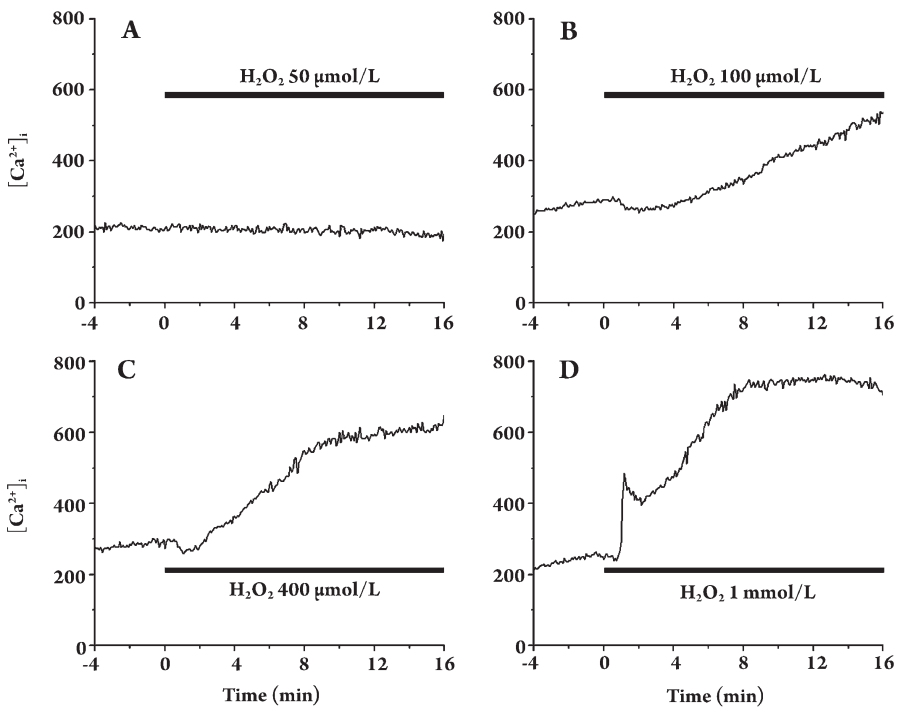


**Figure 1.** $H_2O_2$ elevates $[Ca^{2+}]_i$ across two kinetic patterns in a concentration-dependent manner. In the presence of 1 mmol/L $Ca^{2+}$ in the extracellular solution, $H_2O_2$ was applied to recorded hepatocytes at the concentrations of 50 μmol/L (A), 100 μmol/L (B), 400 μmol/L (C) and 1 mmol/L (D), and the effects on $[Ca^{2+}]_i$ were evaluated. The horizontal bar in each trace indicates the exposure period to $H_2O_2$. Representative traces are typical case from 5–12 experiments tested.

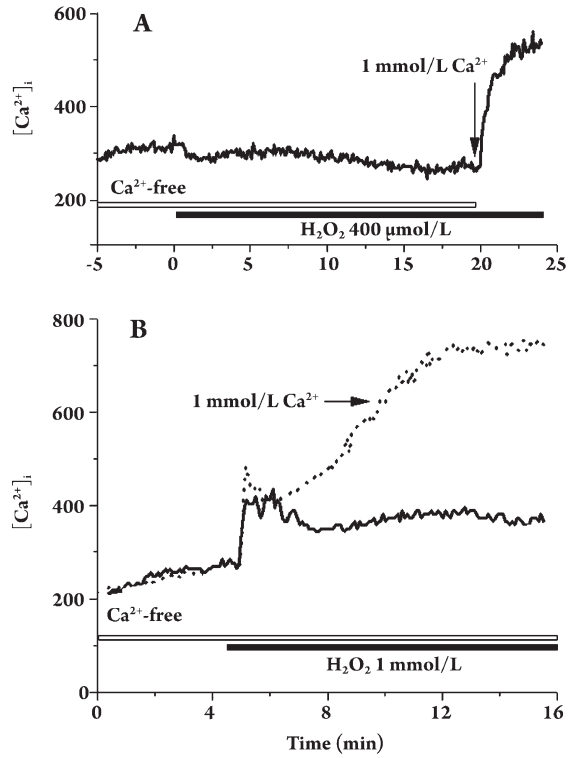


**Figure 2**. Effects of removal of extracellular $Ca^{2+}$ on $H_2O_2$-induced elevation of $[Ca^{2+}]_i$. (A) Under extracellular $Ca^{2+}$-free conditions (open horizontal bar), 400 μmol/L $H_2O_2$ failed to induce a detectable elevation of $[Ca^{2+}]_i$, and the reperfusion of 1 mmol/L extracellular $Ca^{2+}$ (indicated by arrow) induced an elevation of $[Ca^{2+}]_i$. (B) Under the same extracellular $Ca^{2+}$-free conditions, 1 mmol/L $H_2O_2$ still induced a transient, initial elevation of $[Ca^{2+}]_i$, but the sustained phase of elevation of $[Ca^{2+}]_i$ was abolished. The dashed trace represents 1 mmol/L $H_2O_2$-induced elevation of $[Ca^{2+}]_i$ in the presence of 1 mmol/L extracellular $Ca^{2+}$. Representative traces in (A) and (B) are typical cases from 6–9 experiments.

we performed a series of experiments. First, we tested for the existence of ATP-sensitive channels in rat hepatocytes. Under perforated whole-cell patch-clamp recording conditions (pipette solution contained no ATP), voltage-step pulse-induced membrane currents were substantially increased by switching the recording mode from perforated to conventional whole-cell recording, suggesting that reducing intracellular ATP enhances voltage-step pulse-induced membrane currents (Figure 4A). To avoid enhancing membrane currents via a decrease in access resistance (Ra) by converting to conventional whole-cell recording, we compared voltage-step pulse-induced membrane currents using conventional whole-cell recordings at different time points. Under this experimental condition, Ra values were the same at different time points during whole-cell recordings. Voltage-step pulse-induced membrane currents were significantly enhanced 5 min after whole-cell formation compared to 1 min (Figure 4B), thereby supporting the notion that reducing intracellular ATP enhances voltage-step pulse-induced membrane currents. To provide direct evidence that rat hepatocytes contain ATP-sensitive non-selective cation channels, we artificially removed ATP from the space inside the cell during inside-out patch recording, and we investigated whether this manipulation increased membrane current. The removal of ATP increased voltage-ramp pulse-induced membrane currents (Figure 4C). The non-specific cation channel blocker amiloride (1 mmol/L), but not the ATP-sensitive $K^+$ channel blocker tolbutamide (data not shown), mitigated ATP-free induced membrane current increases (Figure 4C). These results further support the existence of ATP-sensitive non-specific cation channels in rat hepatocytes.

**Oxidation is involved in $H_2O_2$-induced membrane current enhancement and $[Ca^{2+}]_i$ elevation** Considering that $H_2O_2$ may impair intracellular ATP production through an oxidation mechanism, we tested the effects of the anti-oxidant melatonin on $H_2O_2$-induced membrane current increases. As shown in Figure 5A, 10 μmol/L melatonin alone did not influence membrane currents, while pre-treatment of hepatocytes with 10 μmol/L melatonin for 3 min followed by co-application of 400 μmol/L $H_2O_2$ plus melatonin failed to induce membrane current increases (Figure 5B). These results suggest that 400 μmol/L $H_2O_2$ may reduce intracellular ATP production through oxidative stress, in turn leading to the opening of ATP-sensitive cation channels, resulting in $Ca^{2+}$ influx through these channels and thereby elevating intracellular $Ca^{2+}$ levels.

**The effect of amiloride on $H_2O_2$-induced changes in membrane conductance and $[Ca^{2+}]_i$** Figure 6A shows whole-cell currents established by the amphotericin B-perforation method. In the presence of 100 μmol/L amiloride, $H_2O_2$ resulted in only a small increase in $[Ca^{2+}]_i$ (Figure 6Ba), while 1 mmol/L amiloride abolished the effects of $H_2O_2$ (Figure 6Ab,c; Bb). In these experiments, we found that the amiloride itself reduced intracellular $Ca^{2+}$ level, but the mechanism of this direct effect of amiloride is unclear. Figure 6Bc summarizes the effects of amiloride on $H_2O_2$ (400 μmol/L)-induced increases in $[Ca^{2+}]_i$ and suggests that $H_2O_2$ (400 μmol/L)-induced increases in both current magnitudes and $[Ca^{2+}]_i$ are mediated via the opening of ATP-sensitive non-specific cation channels.

**$H_2O_2$ reduces intracellular ATP by impairing the mitochondrial function of rat hepatocytes** We then addressed the question of how $H_2O_2$ (400 μmol/L) reduced the intracellular ATP concentration via oxidative mechanisms. One possible hypothesis is that $H_2O_2$ induces oxidation-

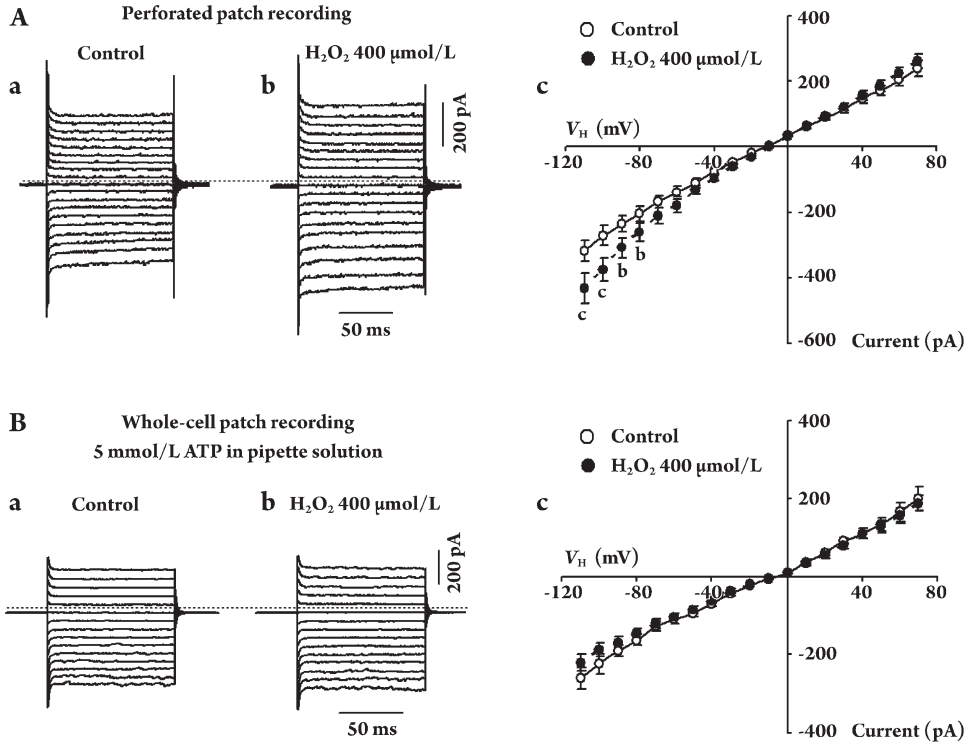


**Figure 3**. Effects of $H_2O_2$ on membrane currents of hepatocytes. (A) Amphotericin B-perforated whole-cell membrane currents induced by 10 mV-increasing and decreasing voltage-step pulses before (a) and during (b) application of 400 μmol/L $H_2O_2$. The holding potential was -20 mV (horizontal dashed line). Ac: Current-voltage relationships obtained from the data presented in (Aa,b) before (○) and during (●) application of $H_2O_2$. (B) Whole-cell membrane currents recorded using the conventional whole-cell method. The pipette solution contained 5 mmol/L ATP. Bc: Current-voltage relationships obtained from the data presented in (Ba,b) before (○) and during (●) application of $H_2O_2$. Representative traces from 5 experiments are shown in (A) and (B). $^bP<0.05$, $^cP<0.01$ before application of $H_2O_2$, respectively.

related mitochondrial dysfunction, which leads to a decrease in ATP production. To test this hypothesis, we monitored inner mitochondrial membrane potential using Rh123 fluorescence imaging and determined the cellular content of NAD(P)H in the mitochondrial pool using NAD(P)H fluorescence imaging. First, we examined the effect of the classic mitochondrial toxin NaCN on mitochondrial membrane potential and NAD(P)H content. NaCN (1 mmol/L) increased Rh123 intensity (Figure 7A) but decreased NAD(P)H autofluorescence intensity (Figure 7B), indicating that it decreased the inner mitochondrial membrane potential (ie, depolarization) and decreased NAD(P)H in the mitochondrial pool[22]. Then, we compared the effect of $H_2O_2$ (400 μmol/L) to 1 mmol/L NaCN. Similar to NaCN, $H_2O_2$ (400 μmol/L) also increased Rh123 intensity (Figure 7A, C) and decreased NAD(P)H autofluorescence intensity (Figure 7B, C). Direct measurements of intracellular concentrations of ATP in hepatocytes demonstrated that after exposure for 6 min to 400 μmol/L $H_2O_2$, intracellular ATP concentrations decreased from 25.6±5.2 cpm (before exposure) to 18.4±4.7 (exposure for 3 min, $P<0.05$, $n=5$) and 16.4±3.7 (exposure for 6 min, $P<0.05$, $n=5$) (data not shown). These results suggest that $H_2O_2$ (400 μmol/L) impairs mitochondrial function and consequently reduces intracellular ATP concentrations.

**Role of the PLC pathway in $H_2O_2$-induced transient elevation of $[Ca^{2+}]_i$** Finally, we conducted experiments to determine whether PLC pathway activation was involved in the transient elevation of $[Ca^{2+}]_i$[20] induced by a high concentration (1 mmol/L) of $H_2O_2$ (which was not sensitive to the removal of extracellular $Ca^{2+}$, Figure 2B). As shown in Figure 8A, in the presence of the PLC inhibitor U73122 (1 μmol/L, 5-min pre-treatment), the 1 mmol/L $H_2O_2$-induced transient (but not sustained) elevation of $[Ca^{2+}]_i$ was eliminated, suggesting that PLC pathway activation does contribute to $H_2O_2$-induced transient elevation of $[Ca^{2+}]_i$. To further confirm the role of PLC activation in 1 mmol/L $H_2O_2$-induced transient elevation of $[Ca^{2+}]_i$, we also directly measured the effect of 1 mmol/L $H_2O_2$ on PLC activity. Figure 8B demonstrates that 1 mmol/L, but not 400 μmol/L

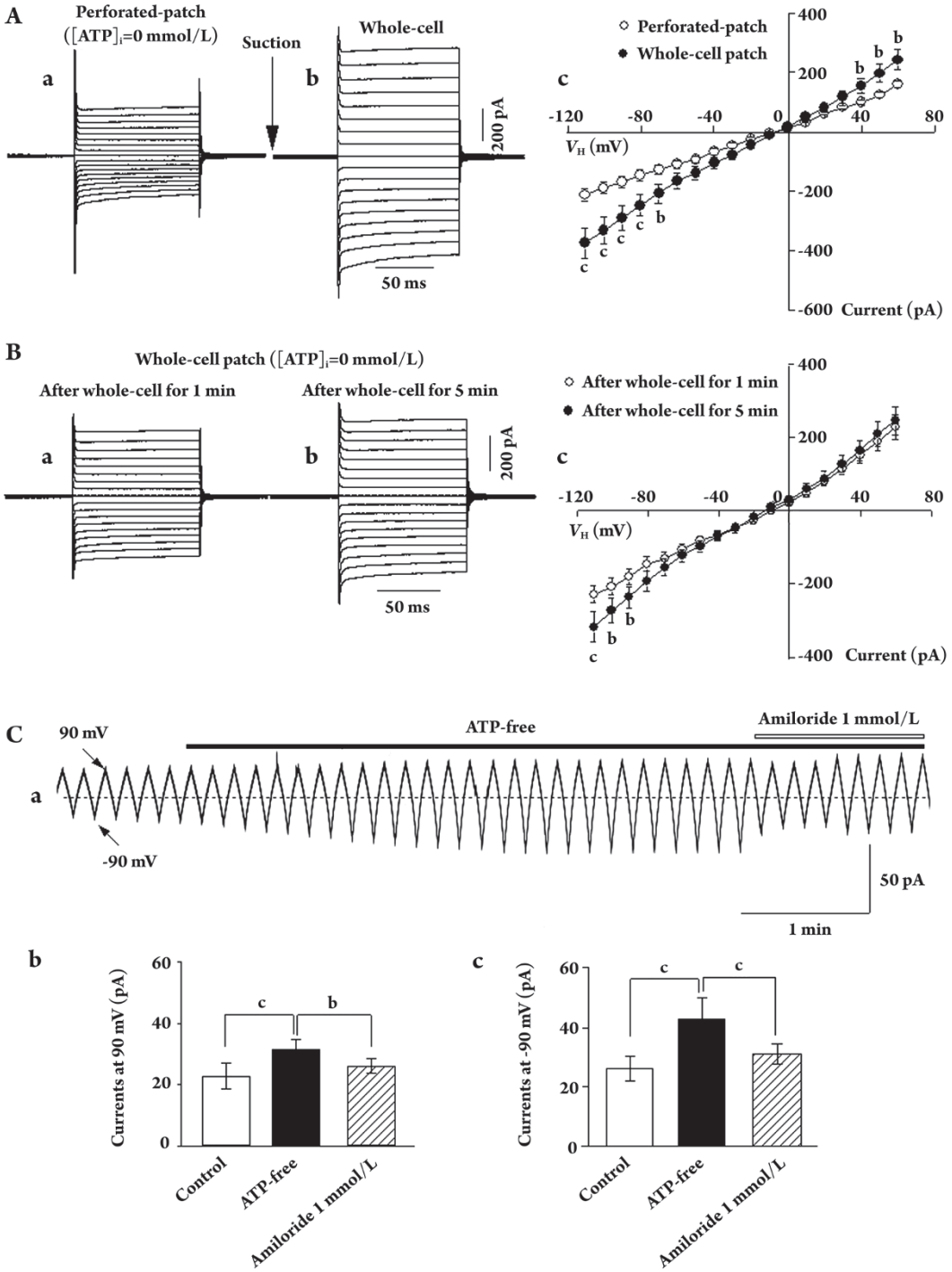


**Figure 4**. ATP-sensitive conductance in hepatocytes. (A) Under perforated-patch conditions with ATP-free pipette solution, step-pulse-induced currents (a) were enhanced by conversion (suction) to conventional whole-cell configuration (b,c). (B) Under whole-cell patch conditions with ATP-free pipette solution, step-pulse-induced currents were tested at 1 (a) and 5 (b) min after conversion to whole-cell conditions and showed an enhancement of membrane currents (c). (C) Inside-out patch recordings. Currents through the membrane in response to repeatedly applied voltage-ramp pulses from -90 to 90 mV are shown (a). Initially, the concentration of ATP in the bath solution was 1 mmol/L, and then ATP was removed and an ATP-free bath solution was used. Amiloride (1 mmol/L) was applied under ATP-free conditions. Representative traces from 5 experiments are shown. The magnitudes of currents were measured at 90 mV (b) and -90 mV (c) of the transmembrane potential. Each column represents the mean from 5 series of experiments. $^{b}P<0.05$, $^{c}P<0.01$.

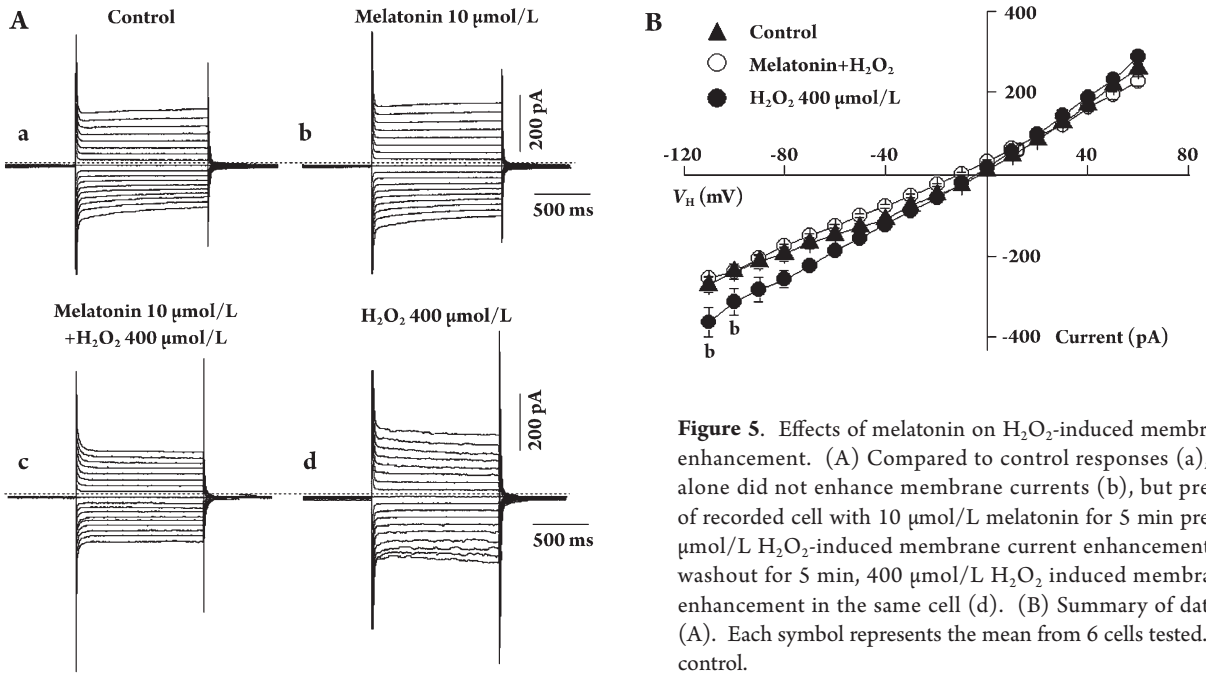


**Figure 5**. Effects of melatonin on $H_2O_2$-induced membrane current enhancement. (A) Compared to control responses (a), melatonin alone did not enhance membrane currents (b), but pre-treatment of recorded cell with 10 μmol/L melatonin for 5 min prevented 400 μmol/L $H_2O_2$-induced membrane current enhancement (c). After washout for 5 min, 400 μmol/L $H_2O_2$ induced membrane current enhancement in the same cell (d). (B) Summary of data shown in (A). Each symbol represents the mean from 6 cells tested. $^bP<0.05$ *vs* control.

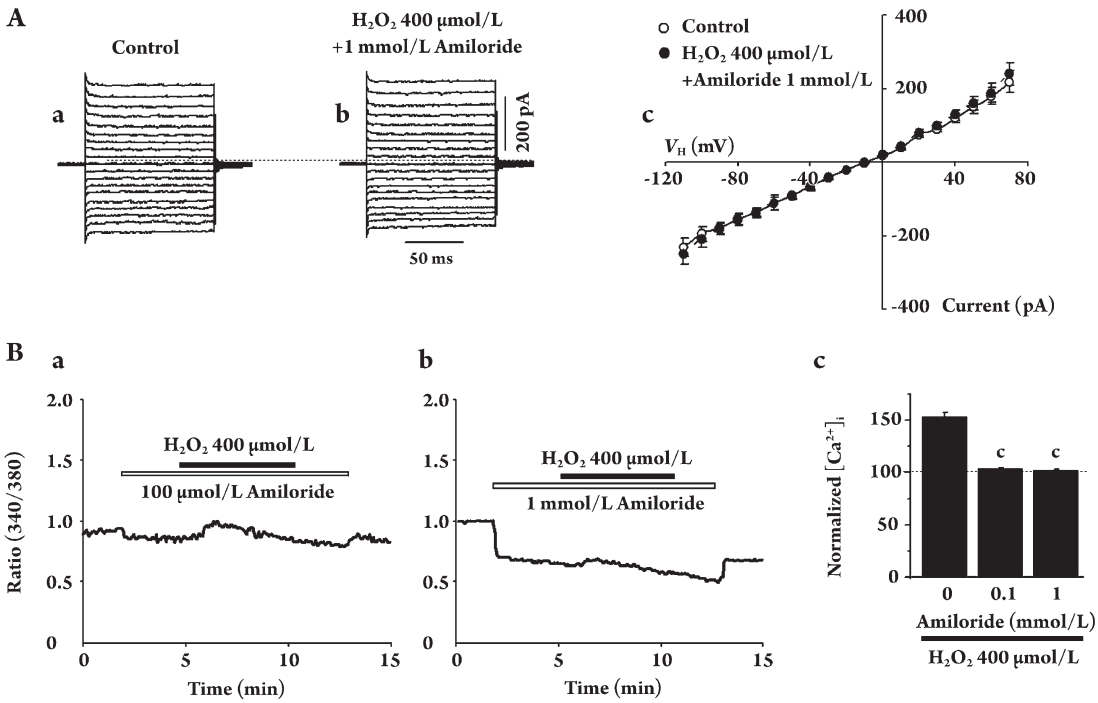


**Figure 6**. Effects of amiloride on $H_2O_2$-induced changes in membrane conductance and $[Ca^{2+}]_i$. (A) Amphotericin B-perforated whole-cell currents recorded in the presence of 1 mmol/L amiloride before (a) and during (b) application of 400 μmol/L $H_2O_2$. Ac: Current-voltage relationships from the data ($n$=6) shown in (Aa,b) before (○) and during (●) application of $H_2O_2$. Ba: $[Ca^{2+}]_i$ was measured in the presence of amiloride (100 μmol/L), and then 400 μmol/L $H_2O_2$ was applied. Bb: The concentration of amiloride was 1 mmol/L. Bc: Normalized $[Ca^{2+}]_i$ from the data of 4–8 experiments shown in (Ba) and (Bb). Application of amiloride by itself caused a decrease in the Fura-2 intensity ratio. The change in the baseline level (Fura-2 intensity ratio) by amiloride seems to be due to some non-specific, direct reversible effect of amiloride on Fura-2 activity because both the appearance and disappearance of the effect are very quick. $^cP<0.01$ *vs* Amiloride 0 mmol/L.

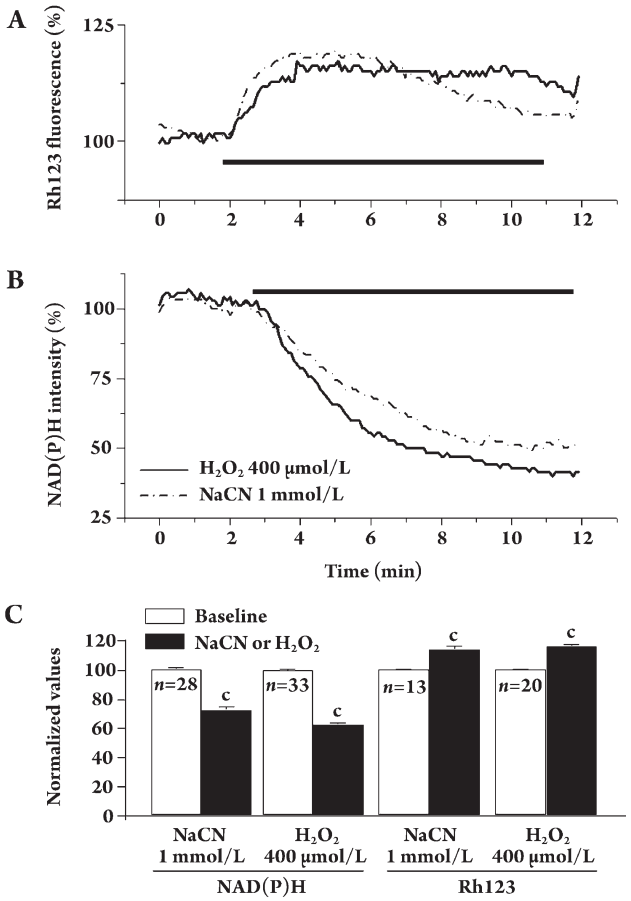


**Figure 7**. $H_2O_2$ impaired mitochondrial function. (A) Rh123 intensity changes induced by 1 mmol/L NaCN (dashed line) and 400 μmol/L $H_2O_2$ (bold line). (B) NAD(P)H intensity changes induced by 1 mmol/L NaCN (dashed line) and 400 μmol/L $H_2O_2$ (bold line). (C) Summary of the effects of 1 mmol/L NaCN and 400 μmol/L $H_2O_2$ on NAD(P)H and Rh123. Baseline values were measured at the 2-min time point and the NaCN-induced and $H_2O_2$-induced responses were measured at the 4-min time point for Rh123 intensity and at the 8-min time point for NAD(P)H intensity. Representative columns from 13–33 cells tested. $^cP<0.01$ *vs* baseline.

$H_2O_2$, increased PLC activity, supporting the hypothesis that PLC activation-induced mobilization of $Ca^{2+}$ from intracellular $Ca^{2+}$ stores underlies 1 mmol/L $H_2O_2$-induced transient elevation of $[Ca^{2+}]_i$. Theoretically, PLC pathway activation produces $IP_3$, which mobilizes $Ca^{2+}$ from $IP_3$-induced $Ca^{2+}$ release (IICR), while released $Ca^{2+}$ from IICR also can trigger the $Ca^{2+}$-induced $Ca^{2+}$ release (CICR) mechanism. To test whether ryanodine-sensitive $Ca^{2+}$ stores play a role in generating 1 mmol/L $H_2O_2$-induced transient elevation of $[Ca^{2+}]_i$, we examined the effects of 100 μmol/L ryanodine on the 1 mmol/L $H_2O_2$-induced transient elevation of $[Ca^{2+}]_i$. Our results demonstrated that pretreatment with 100 μmol/L ryanodine for 2 min failed to abolish 1 mmol/L $H_2O_2$-induced transient elevation of $[Ca^{2+}]_i$ (supplemental Figure 1). This suggests that ryanodine-sensitive $Ca^{2+}$ stores may not play an important role in generating the 1 mmol/L $H_2O_2$-induced transient elevation of $[Ca^{2+}]_i$.

## Discussion

Our study's major contribution is the identification of two distinct mechanisms of $[Ca^{2+}]_i$ elevation induced by $H_2O_2$. Low-concentration (400 μmol/L) $H_2O_2$-induced sustained $[Ca^{2+}]_i$ elevation is mediated through a $Ca^{2+}$ influx mechanism, in which $H_2O_2$ impairs mitochondrial function, reduces intracellular ATP production, opens ATP-sensitive, non-specific cation channels, and leads to $Ca^{2+}$ influx. An increase in the $H_2O_2$ concentration to 1 mmol/L induced an additional, transient elevation of $[Ca^{2+}]_i$, which is mediated through activation of the PLC signaling pathway followed by mobilization of $Ca^{2+}$ from intracellular $Ca^{2+}$ stores.

**$H_2O_2$ elevates $[Ca^{2+}]_i$ consistent with two dynamic patterns, which are mediated through distinct mechanisms** Our research suggests that acute exposure to $H_2O_2$

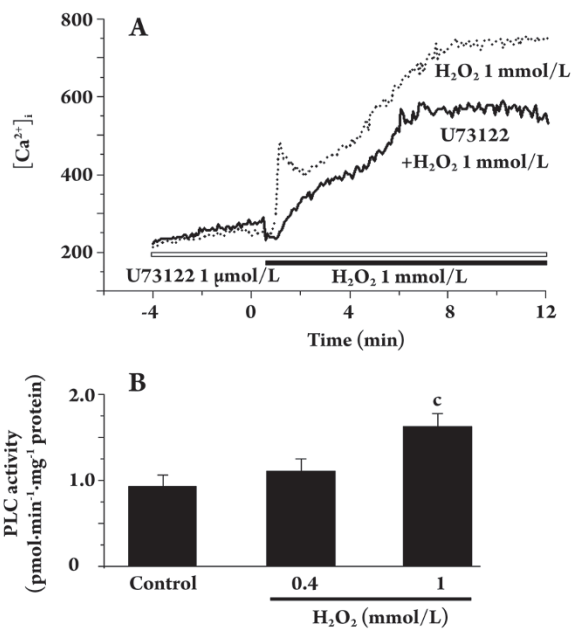


**Figure 8**. Role of the PLC pathway in $H_2O_2$-induced elevation of $[Ca^{2+}]_i$. (A) Hepatocytes were pre-treated with 1 μmol/L U73122 for 30 min and then stimulated with 1 mmol/L $H_2O_2$ in the presence of 1 mmol/L $Ca^{2+}$. (B) Direct measurements of PLC activity during exposure to different concentrations of $H_2O_2$ showed that only 1 mmol/L $H_2O_2$ significantly increased PLC activity. Each column represents the average from 5 experiments and the vertical bars represent SD. $^cP<0.01$ *vs* control.

mobilizes $Ca^{2+}$ from rat hepatocytes via two distinct mechanisms: $Ca^{2+}$ entry from the extracellular space and $Ca^{2+}$ release from intracellular stores. In many other cell types, these two mechanisms are often linked. For instance, in exocrine cells, agonists induce $Ca^{2+}$ release first from intracellular $Ca^{2+}$ stores triggered by $IP_3$ produced via a membrane receptor-PLC-linked signal transduction cascade[24], and then the emptied $Ca^{2+}$ stores mediate the opening of $Ca^{2+}$-permeable channels in the cell membrane[25, 26]. In this case, lower concentrations of the agonist cause only $Ca^{2+}$ release from stores, and at higher concentrations or with long-time exposure to low concentrations of the agonist, the phase reflective of the $Ca^{2+}$ influx appears[26]. On the other hand, in cardiac myocytes and smooth muscle cells, $Ca^{2+}$ entry first occurs through voltage-gated $Ca^{2+}$ channels that are opened by depolarizing stimuli. The incoming $Ca^{2+}$ triggers $Ca^{2+}$ release from the sarcoplasmic reticulum, thereby activating ryanodine-sensitive $Ca^{2+}$ channels in the sarcoplasmic reticulum membrane[27]. In the present study, the concentrations of $H_2O_2$ were relatively high (0.4 and 1 mmol/L). We chose these concentrations on the basis of published literature and our previous results. It has been reported that high concentrations of $H_2O_2$ (>1 mmol/L) are necessary to induce apoptosis of liver cells[28]. In addition, Lu and Tian reported[17] that exposure of liver cells to 10 mmol/L $H_2O_2$ for 2 h induced cell apoptosis through intracellular $Ca^{2+}$ overloading. In the present study, the results (Figure 1) clearly showed that $H_2O_2$ induced a strong and sustained $Ca^{2+}$ elevation at the concentration of 400 μmol/L. In particular, 1 mmol/L of $H_2O_2$ was required to induce the transient $Ca^{2+}$ component (Figure 1D), and also to increase PLC activity (Figure 8B). Accordingly, for the purpose of studying the mechanisms of acute $H_2O_2$-induced sustained and transient $Ca^{2+}$ signals in liver cells, the $H_2O_2$ concentrations used in the present study were appropriate.

**$Ca^{2+}$ entry induced by $H_2O_2$ occurs through the opening of ATP-sensitive non-specific cation channels** Although hepatocytes have no voltage-gated $Ca^{2+}$ channels, various pathways for $Ca^{2+}$ entry have been proposed in rat and guinea-pig hepatocytes. For instance, hepatocytes possess non-specific cation channels that are permeable to $Na^+$, $K^+$, and $Ca^{2+}$ [29], and these types of channels are activated by membrane stretch[29] and externally applied ATP[30]. Various hormones, including hepatocyte growth factor[31], vasopressin[32], insulin[33], and norepinephrine[10], have been reported to activate $Ca^{2+}$-permeable channels. In addition, hepatocytes possess $Ca^{2+}$ release-activated $Ca^{2+}$ channels[4, 34, 35]. Membrane currents through $Ca^{2+}$ release-activated $Ca^{2+}$ channels ($I_{CRAC}$) can be recorded in intact hepatocytes[35], and both ATP and vasopressin can activate $I_{CRAC}$[36], suggesting that this type of channel is capable of being opened without altering the volume of $Ca^{2+}$ stores. In addition, the transient receptor potential canonical 1 protein has been shown to form a $Ca^{2+}$-permeable non-specific cation channel responsible for both store depletion-induced $Ca^{2+}$ entry and cell volume regulation in liver cells[37]. In L02 cells (a human hepatic cell clone), $I_{CRAC}$-linked Fas protein was expressed by Fas mRNA transduction, and $H_2O_2$ promoted $Ca^{2+}$ influx, which was responsible for cell apoptosis[17]. Further studies are required to elucidate the characteristic similarities of the non-specific cation channels and Fas protein.

In our study, $H_2O_2$-induced $Ca^{2+}$ influx through non-specific cation channels may be related to a possible decrease in the concentration of intracellular ATP. The action of ATP on non-specific cation channels differs at sites where ATP is utilized and across cell types. As mentioned previously, extracellular ATP activates non-specific cation channels in hepatocytes[30, 36]. A similar effect induced by extracellular ATP has been shown in basophilic leukemia cells[38]. Non-specific cation channels that are inhibited by intracellular ATP (or activated by a decrease in intracellular ATP concentration) have been identified in a number of cell types[39–41]. Thus, it is possible that ATP-sensitive non-specific cation channels are expressed in hepatocytes, and our data showing that the removal of intracellular ATP increases membrane currents (Figure 4) supports this hypothesis. However, to date no selective antagonists are available to further characterize these ATP-sensitive non-specific cation channels.

**$H_2O_2$ impairs mitochondrial function and decreases intracellular ATP concentrations** The results shown in Figure 7 indicate that $H_2O_2$ impairs hepatocyte mitochondrial function, which in turn results in a decreased intracellular ATP concentration. Oxidative stress induced by oxygen and nitrogen species is known to cause cell injury and/or death, particularly by impairing mitochondrial function. Oxygen radicals are produced by mitochondria, and those produced in other cells can easily enter a target cell via the cell membrane and thereby reach the interior of mitochondria. The mechanisms by which oxygen radicals impair mitochondrial function involve mitochondrial membrane permeability transitions[16] and mitochondrial DNA damage[42], leading to cell death. In such processes, mitochondrial and cytosolic $Ca^{2+}$ likely play important roles. In fact, reactive oxygen and nitrogen species regulate mitochondrial $Ca^{2+}$ homeostasis[23], and impairment of mitochondrial function is also dependent on $Ca^{2+}$ [43]. In neurons, $Ca^{2+}$-dependent mitochondrial dysfunction is known to result in the release of apoptogenic

proteins from mitochondria, thereby leading to cell death[44]. Furthermore, impaired mitochondrial function leads to a loss of ATP synthesis[45].

## Acknowledgments

This work was supported by a Grant-in-Aid for scientific research from the Japan Ministry of Education, Science, Sports, and Culture to Dr Makoto WAKUI (1247005).

The authors thank Kevin ELLSWORTH for his assistance in preparing this article.

## Author contribution

Hirohiko SATO, Qiang LIU: perform patch-clamp experiments and data analysis. Teruko TAKEO, Sechiko SUGA: perform $Ca^{2+}$ image experiments and data analysis. Kyoko NAKANO, Tomohiro OSANAI: perform biochemical experiments and data analysis. Makoto WAKUI, Jie WU: design experiments, analyze data and write the manuscript.

## Abbreviations

$H_2O_2$, hydrogen peroxide; OH·, hydroxyl radical; $O^{2-}$, superoxide anion; PLC, phospholipase C; $IP_3$, inositol trisphosphate; rhodamine 123, (Rh123); SR, sarcoplasmic reticulum

## References

1 Bzeizi KI, Dawkes R, Dodd NJ, Plevris JN, Hayes PC. Graft dysfunction following liver transplantation: role of free radicals. J Hepatol 1997; 26: 69–74.
2 Jaeschke H. Mechanisms of liver injury. II. Mechanisms of neutrophil-induced liver cell injury during hepatic ischemia-reperfusion and other acute inflammatory conditions. Am J Physiol Gastrointest Liver Physiol 2006; 290: G1083–8.
3 Rosser BG, Gores GJ. Liver cell necrosis: cellular mechanisms and clinical implications. Gastroenterology 1995; 108: 252–75.
4 Rychkov G, Brereton HM, Harland ML, Barritt GJ. Plasma membrane $Ca^{2+}$ release-activated $Ca^{2+}$ channels with a high selectivity for $Ca^{2+}$ identified by patch-clamp recording in rat liver cells. Hepatology 2001; 33: 938–47.
5 Hoffman JW Jr, Gilbert TB, Poston RS, Silldorff EP. Myocardial reperfusion injury: etiology, mechanisms, and therapies. J Extra Corpor Technol 2004; 36: 391–411.
6 Slater TF. Free-radical mechanisms in tissue injury. Biochem J 1984; 222: 1–15.
7 Conde de la Rosa L, Schoemaker MH, Vrenken TE, Buist-Homan M, Havinga R, Jansen PL, *et al.* Superoxide anions and hydrogen peroxide induce hepatocyte death by different mechanisms: involvement of JNK and ERK MAP kinases. J Hepatol 2006; 44: 918–29.
8 Hinshaw DB, Miller MT, Omann GM, Beals TF, Hyslop PA. A cellular model of oxidant-mediated neuronal injury. Brain Res 1993; 615: 13–26.
9 Starke PE, Hoek JB, Farber JL. Calcium-dependent and calcium-independent mechanisms of irreversible cell injury in cultured hepatocytes. J Biol Chem 1986; 261: 3006–12.
10 Nagano T, Sato R, Matsuda H, Aramaki T. Evidence for norepinephrine-activated $Ca^{2+}$ permeable channels in guinea-pig hepatocytes using a patch clamp technique. Nippon Ika Daigaku Zasshi 1999; 66: 127–33.
11 Arundine M, Tymianski M. Molecular mechanisms of calcium-dependent neurodegeneration in excitotoxicity. Cell Calcium 2003; 34: 325–37.
12 Klonowski-Stumpe H, Schreiber R, Grolik M, Schulz HU, Haussinger D, Niederau C. Effect of oxidative stress on cellular functions and cytosolic free calcium of rat pancreatic acinar cells. Am J Physiol 1997; 272: G1489–98.
13 Kilpatrick LE, Jakabovics E, McCawley LJ, Kane LH, Korchak HM. Cromolyn inhibits assembly of the NADPH oxidase and superoxide anion generation by human neutrophils. J Immunol 1995; 154: 3429–36.
14 Meyer TN, Gloy J, Hug MJ, Greger R, Schollmeyer P, Pavenstadt H. Hydrogen peroxide increases the intracellular calcium activity in rat mesangial cells in primary culture. Kidney Int 1996; 49: 388–95.
15 Levitsky J, Gurell D, Frishman WH. Sodium ion/hydrogen ion exchange inhibition: a new pharmacologic approach to myocardial ischemia and reperfusion injury. J Clin Pharmacol 1998; 38: 887–97.
16 Battaglia V, Salvi M, Toninello A. Oxidative stress is responsible for mitochondrial permeability transition induction by salicylate in liver mitochondria. J Biol Chem 2005; 280: 33864–72.
17 Lu QP, Tian L. Fas mRNA expression and calcium influx change in H2O2-induced apoptotic hepatocytes *in vitro*. World J Gastroenterol 2005; 11: 534–7.
18 Rooney TA, Sass EJ, Thomas AP. Characterization of cytosolic calcium oscillations induced by phenylephrine and vasopressin in single fura-2-loaded hepatocytes. J Biol Chem 1989; 264: 17131–41.
19 Jackowski S, Rettenmier CW, Sherr CJ, Rock CO. A guanine nucleotide-dependent phosphatidylinositol 4,5-diphosphate phospholipase C in cells transformed by the v-fms and v-fes oncogenes. J Biol Chem 1986; 261: 4978–85.
20 Suga S, Nakano K, Takeo T, Osanai T, Ogawa Y, Yagihashi S, *et al.* Masked excitatory action of noradrenaline on rat islet beta-cells via activation of phospholipase C. Pflugers Arch 2003; 447: 337–44.
21 Maechler P, Kennedy ED, Pozzan T, Wollheim CB. Mitochondrial activation directly triggers the exocytosis of insulin in permeabilized pancreatic beta-cells. EMBO J 1997; 16: 3833–41.
22 Duchen MR, Smith PA, Ashcroft FM. Substrate-dependent changes in mitochondrial function, intracellular free calcium concentration and membrane channels in pancreatic beta-cells. Biochem J 1993; 294: 35–42.
23 Richter C. Reactive oxygen and nitrogen species regulate mitochondrial $Ca^{2+}$ homeostasis and respiration. Biosci Rep 1997; 17: 53–66.
24 Petersen OH. $Ca^{2+}$ signalling and $Ca^{2+}$-activated ion channels in exocrine acinar cells. Cell Calcium 2005; 38: 171–200.

25 Parekh AB, Putney JW Jr. Store-operated calcium channels. Physiol Rev 2005; 85: 757–810.
26 Putney JW. Physiological mechanisms of TRPC activation. Pflugers Arch 2005; 451: 29–34.
27 Kamishima T, Quayle JM. $Ca^{2+}$-induced $Ca^{2+}$ release in cardiac and smooth muscle cells. Biochem Soc Trans 2003; 31: 943–6.
28 Xu Y, Bradham C, Brenner DA, Czaja MJ. Hydrogen peroxide-induced liver cell necrosis is dependent on AP-1 activation. Am J Physiol 1997; 273: G795–803.
29 Bear CE. A nonselective cation channel in rat liver cells is activated by membrane stretch. Am J Physiol 1990; 258: C421–8.
30 Bear CE, Li CH. Calcium-permeable channels in rat hepatoma cells are activated by extracellular nucleotides. Am J Physiol 1991; 261: C1018–24.
31 Baffy G, Yang L, Michalopoulos GK, Williamson JR. Hepatocyte growth factor induces calcium mobilization and inositol phosphate production in rat hepatocytes. J Cell Physiol 1992; 153: 332–9.
32 Duszynski J, Elensky M, Cheung JY, Tillotson DL, LaNoue KF. Hormone-regulated $Ca^{2+}$ channel in rat hepatocytes revealed by whole cell patch clamp. Cell Calcium 1995; 18: 19–29.
33 Benzeroual K, van de Werve G, Meloche S, Mathe L, Romanelli A, Haddad P. Insulin induces $Ca^{2+}$ influx into isolated rat hepatocyte couplets. Am J Physiol 1997; 272: G1425–32.
34 Gregory RB, Barritt GJ. Evidence that $Ca^{2+}$-release-activated $Ca^{2+}$ channels in rat hepatocytes are required for the maintenance of hormone-induced $Ca^{2+}$ oscillations. Biochem J 2003; 370: 695–702.
35 Zhou HY, Wang F, Cheng L, Fu LY, Zhou J, Yao WX. Effects of tetrandrine on calcium and potassium currents in isolated rat hepatocytes. World J Gastroenterol 2003; 9: 134–6.
36 Rychkov GY, Litjens T, Roberts ML, Barritt GJ. ATP and vasopressin activate a single type of store-operated $Ca^{2+}$ channel, identified by patch-clamp recording, in rat hepatocytes. Cell Calcium 2005; 37: 183–91.
37 Chen J, Barritt GJ. Evidence that TRPC1 (transient receptor potential canonical 1) forms a $Ca^{2+}$-permeable channel linked to the regulation of cell volume in liver cells obtained using small interfering RNA targeted against TRPC1. Biochem J 2003; 373: 327–36.
38 Obukhov AG, Jones SV, Degtiar VE, Luckhoff A, Schultz G, Hescheler J. $Ca^{2+}$-permeable large-conductance nonselective cation channels in rat basophilic leukemia cells. Am J Physiol 1995; 269: C1119–25.
39 Chen M, Simard JM. Cell swelling and a nonselective cation channel regulated by internal $Ca^{2+}$ and ATP in native reactive astrocytes from adult rat brain. J Neurosci 2001; 21: 6512–21.
40 Hurwitz CG, Hu VY, Segal AS. A mechanogated nonselective cation channel in proximal tubule that is ATP sensitive. Am J Physiol Renal Physiol 2002; 283: F93–F104.
41 Ono S, Mougouris T, DuBose TD Jr, Sansom SC. ATP and calcium modulation of nonselective cation channels in IMCD cells. Am J Physiol 1994; 267: F558–65.
42 Van Houten B, Woshner V, Santos JH. Role of mitochondrial DNA in toxic responses to oxidative stress. DNA Repair (Amst) 2006; 5: 145–52.
43 Murphy AN. $Ca^{2+}$-mediated mitochondrial dysfunction and the protective effects of Bcl-2. Ann N Y Acad Sci 1999; 893: 19–32.
44 Fiskum G. Mitochondrial participation in ischemic and traumatic neural cell death. J Neurotrauma 2000; 17: 843–55.
45 Ballinger SW, Patterson C, Yan CN, Doan R, Burow DL, Young CG, *et al.* Hydrogen peroxide- and peroxynitrite-induced mitochondrial DNA damage and dysfunction in vascular endothelial and smooth muscle cells. Circ Res 2000; 86: 960–6.